ACS Chemical Neuroscience

Subscriber access provided by MINCyT

Article

Functionalization and characterization of magnetic nanoparticles for the detection of ferritin accumulation in Alzheimer's disease

Tamara Fernández, Alberto Martínez-Serrano, Lorena Cussó, Manuel Desco, and Milagros Ramos-Gómez

ACS Chem. Neurosci., **Just Accepted Manuscript** • DOI: 10.1021/acschemneuro.7b00260 • Publication Date (Web): 03 Jan 2018

Downloaded from http://pubs.acs.org on January 17, 2018

Just Accepted

"Just Accepted" manuscripts have been peer-reviewed and accepted for publication. They are posted online prior to technical editing, formatting for publication and author proofing. The American Chemical Society provides "Just Accepted" as a free service to the research community to expedite the dissemination of scientific material as soon as possible after acceptance. "Just Accepted" manuscripts appear in full in PDF format accompanied by an HTML abstract. "Just Accepted" manuscripts have been fully peer reviewed, but should not be considered the official version of record. They are accessible to all readers and citable by the Digital Object Identifier (DOI®). "Just Accepted" is an optional service offered to authors. Therefore, the "Just Accepted" Web site may not include all articles that will be published in the journal. After a manuscript is technically edited and formatted, it will be removed from the "Just Accepted" Web site and published as an ASAP article. Note that technical editing may introduce minor changes to the manuscript text and/or graphics which could affect content, and all legal disclaimers and ethical guidelines that apply to the journal pertain. ACS cannot be held responsible for errors or consequences arising from the use of information contained in these "Just Accepted" manuscripts.

ACS Publications

ACS Chemical Neuroscience is published by the American Chemical Society. 1155 Sixteenth Street N.W., Washington, DC 20036

Published by American Chemical Society. Copyright © American Chemical Society. However, no copyright claim is made to original U.S. Government works, or works produced by employees of any Commonwealth realm Crown government in the course of their duties.

Functionalization and characterization of magnetic nanoparticles for the detection of ferritin accumulation in Alzheimer's disease

Tamara Fernández[1], Alberto Martínez-Serrano[2], Lorena Cussó[3,4,5], Manuel Desco[3,4,5] and Milagros Ramos-Gómez[1,6,*]

1 Centre for Biomedical Technology (CTB), Universidad Politécnica de Madrid, Spain

2 Department of Molecular Biology and Centre for Molecular Biology "Severo Ochoa" (CBMSO), Universidad Autónoma de Madrid and Consejo Superior de Investigaciones Científicas, Madrid, Spain.

3 Departamento de Ingeniería Biomédica e Ingeniería Aeroespacial, Universidad Carlos III de Madrid, 28911 Leganés, Spain.

4 Instituto de Investigación Sanitaria Gregorio Marañón, 28007 Madrid, Spain.

5 Centro de Investigación Biomédica en Red de Salud Mental (CIBERSAM), 28029 Madrid, Spain

6 CIBER de Bioingeniería, Biomateriales y Nanomedicina (CIBER-BBN), Madrid, Spain.

*Corresponding author

Abstract

Early diagnosis in Alzheimer's disease (AD), prior to the appearance of marked clinical symptoms, is critical to prevent irreversible neuronal damage and neural malfunction that leads to dementia and death. Therefore, there is an urgent need to generate new contrast agents which reveal by a non-invasive method the presence of some of the pathological signs of AD.

In the present study we demonstrate for the first time a new nanoconjugate composed of magnetic nanoparticles bound to an anti-ferritin antibody, which has been developed based on the existence of iron deposits and high levels of the ferritin protein present in areas with a high accumulation of amyloid plaques (particularly the subiculum in the hippocampal area) in the brain of a transgenic mouse model with five familial AD mutations.

Both in vitro and after intravenous injection, functionalized magnetic nanoparticles were able to recognize and bind specifically to the ferritin protein accumulated in the subiculum area of the AD transgenic mice.

Keywords

Iron oxide nanoparticles, nanoconjugates, ferritin, iron deposits, microglia, Alzheimer´s disease.

Introduction

Alzheimer´s disease (AD) is a progressive neurodegenerative disorder, with no known prevention or cure, which affects approximately 47 million patients worldwide[1]. At present, a definitive diagnosis of AD is only possible after the patient's death, when the presence of amyloid plaques and tangles in the brain parenchyma can be revealed by histological examination[2]. Current diagnostic practices, including assessments of clinical history to detect changes in behavior, physical examination, neuropsychiatric testing (Mini-Mental State Examination, MMSE), diagnostic laboratory tests and neuroimaging, can only make a "probable" diagnosis of AD[3].

To date, the best-established biomarkers for the detection and monitoring of AD include measures of ß amyloid peptide and tau in cerebrospinal fluid, hippocampal atrophy as assessed by magnetic resonance imaging (MRI), reduction in the rate of glucose metabolism in the brain, assessed by positron emission tomography (PET) with fluorodeoxyglucose, and brain accumulation of ß amyloid peptide visualized by PET using Pittsburgh Compound B[3],[4]. None of these methods, alone or in combination, provide high accuracy in the early diagnosis of pathology. Therefore, great emphasis has been placed on the search for biomarkers indicative of AD, but most attempts to date have had limited success[5].

With the improvements in imaging technologies in recent years, there has been a growing interest in developing methods to visualize amyloid plaques in AD, especially in transgenic mice, using methods that could eventually be applied to humans[6],[7]. The therapeutic approaches currently developed show that the available therapies are more effective when applied at very early stages, when a low burden of amyloid plaques can be detected[8],[9].Therefore, early diagnosis of the disease is a critical issue.

MRI has a higher spatial resolution than PET in the study of whole brain. MRI is a widely available technique that can produce images in both experimental animals and in patients without the need for a radiotracer[10]. Several groups have been able to visualize amyloid plaques in vivo utilizing both the endogenous contrast induced by the plaques attributed to their iron content and by selectively enhancing the signal from amyloid plaques using molecular-targeting vectors labeled with MRI contrast agents[11],[12]. These data were corroborated using both postmortem brain tissue from AD patients[13], and brain tissue from transgenic AD mice[14],[15],[16].

Histological findings associated with AD show the presence of iron deposits in the vicinity of plaques in the brains of patients with the disease[17],[18]. The intrinsic MRI contrast arising from the iron associated with plaques creates an unexpected opportunity for the noninvasive investigation of the temporal course of development of the plaques in the animal brain, thus reducing intersubject variability[16]. However, the limiting factor of this methodological approach, in which no contrast agent is used, is that only amyloid plaques with a diameter of more than 50

μm can be detected, using acquisition times that generally exceed 2h. These very long times complicate the acquisition of in vivo images, not only in research animals, but also in the clinical setting.

In order to detect amyloid plaques at early stages of the disease, and to diminish the acquisition times of in vivo imaging, several studies have proposed the use of magnetic iron oxide nanoparticles as specific contrast agents for MRI[19,20]. The hypointense effect exhibited by these particles in T2 and T2* image sequences provides greater contrast in MR images. Therefore, the use of magnetic iron oxide nanoparticles (MNPs) may be a good method for the early diagnosis of AD.

Different types of functionalized MNPs have been evaluated in AD models including those coupled to amyloid B peptide 1–40[21], amyloid B peptide 1–30[22], amyloid B peptide 1–42[11] and to peptides highly specific for Aβ amyloid fibrils[23,24]; also by coupling the MNPs to antibodies which specifically recognize amyloid B peptide 1–42 as a component of amyloid plaques[25,26,27,19]. MNPs functionalized with different markers of amyloid plaques, such as Thioflavin S[28], Congo Red[29], 1,1-dicyano-2-[6-(dimethylamino)naphthalene-2-yl] propene (DDNP)[30] and curcumin[31], have also been used to target and detect amyloid plaques in AD transgenic mice using ex vivo MRI with long acquisition times.

The localized iron accumulation and formation of iron deposits in the brain, together with changes in the regulation of iron–storage and the association of iron with several proteins is evident in several neurodegenerative diseases, including AD[32,33]. Proteomic analysis has also shown higher levels of ferritin, the main protein that stores and transports iron in vertebrates, in the hippocampal region of AD patients compared to healthy individuals[34]. Moreover, iron and ferritin are deposited in close proximity to amyloid plaques in the cerebral cortex of AD patients, as determined in post-mortem specimens[35,36].

The present manuscript presents a novel nanoconjugate based on MNPs bound to an anti-ferritin antibody, which could be a useful tool to detect increases in the expression of ferritin in the

brain parenchyma of transgenic mice with five familial Alzheimer's disease mutations (5XFAD) by MRI[37]. This nanoconjugate showed a high specific binding to the ferritin protein present in the subiculum of 5XFAD mice after being injected intravenously, while non-functionalized MNPs could not be detected in the same brain region after injection. The results demonstrated that the functionalization of MNPs with the anti-ferritin antibody generated a specific contrast agent useful for detecting the presence of ferritin in the brain parenchyma of the 5XFAD mice, and consequently the presence of iron deposits in the vicinity of amyloid plaques, one of the hallmarks of AD.

Results and Discussion

We report here a novel method for the selective marking of the protein ferritin, present in areas with a high accumulation of amyloid plaques, with functionalized magnetic nanoparticles. This novel nanoconjugate, which selectively marked ferritin, might be used in the near future as a contrast agent for MRI enabling the noninvasive early detection of AD.

The development of biofunctionalized devices could become a useful tool in diagnosis and therapy of several neuropathologies and become a strategy to deepen knowledge in cell biology and histopathology in neuroscience.

Iron and ferritin accumulation in 5XFAD mice

There is some evidence for altered iron metabolism in AD, including alterations in iron accumulation and changes in transferrin and ferritin levels[17]. Striking iron accumulation has been closely associated with amyloid plaques, neurofibrillary tangles, and neuropil threads in clinical cases of AD[38]. Increased levels of ferritin have also been observed by proteomic analysis within the hippocampal region in AD patients compared to healthy individuals[34]. To determine whether these highly relevant histological findings were also present in 5XFAD mice, the presence of iron was evaluated in 9-month-old 5XFAD transgenic and nontransgenic mice by Prussian blue staining. Brain sections from nontransgenic mice showed no obvious Prussian blue staining, indicating a lack of iron accumulation in the brain (Figure 1A). However, iron

burden was obvious in the subiculum of 5XFAD mice (Figure 1B), an area usually containing a high number of amyloid plaques[37]. In fact, when brain sections were stained with Thioflavin S, a marker of amyloid plaques, a strong signal could be detected in the subiculum area only in the 5XFAD mice (Figure 1D), indicating a high density of amyloid plaques coinciding with the strong accumulation of iron in this hippocampal region. As expected, amyloid protein was not detected in nontransgenic mice (Figure 1C).

Since high iron content was observed in 5XFAD mice in the hippocampal area, we stained similar brain sections with an anti-ferritin antibody to determine the levels of this iron-binding protein in this region. While the presence of this protein in control mice was almost negligible (Figure 1E), in 5XFAD brain sections, strong labeling for ferritin protein was evident in the subiculum (Figure 1F).

This high expression of ferritin in the subiculum of the 5XFAD transgenic mice coincided perfectly with the presence of a high number of amyloid plaques in the same area (arrows in Figure 1D and 1F).

The regional accumulation of iron deposits in the brain, together with changes in the regulation of iron storing proteins and the association of iron with neuropathology is evident in several neurodegenerative diseases, including AD , Parkinson's disease, multiple sclerosis and Huntington's disease, where the accumulation of iron in the brain corresponds to the regions of greatest neuronal degeneration[39-44]. Iron accumulation in these neurodegenerative diseases occurs in different brain regions. In AD, iron accumulation occurs in the hippocampus[40]. In Huntington's disease, an increased iron burden in the cortex and striatum has been shown in both patients and transgenic mouse models for the disease[41]. In patients with Parkinson's disease, accumulation of iron occurs in the substantia nigra[42]. In the case of multiple sclerosis, an increase in iron in the spinal cord white matter has also been described[43]. Therefore, a specific contrast agent able to detect iron deposits by MRI could be useful for the diagnosis of several neurodegenerative diseases. Furthermore, each neurodegenerative disorder could then be distinguished by determining the brain area(s) where such iron accumulations occur. In this

way, the developed nanoconjugate would be a useful tool to detect AD, depending on the location of the iron accumulations in the brain.

Iron deposits and a strong immunoreactivity for ferritin have been observed near the amyloid plaques in the cortex and in the hippocampus of AD patients[35,36]. Ferritin accumulation was almost exclusively associated with reactive microglial cells, which appeared to have greatly proliferated[36]. To determine if iron and ferritin accumulations in 5XFAD mice were deposited close to the amyloid plaques, a double staining was performed using an antibody specific for the ferritin protein and a specific marker for amyloid plaques (Thioflavin S). Cells labeled with the anti-ferritin antibody were found near the amyloid plaques, with their processes in close contact with and surrounding the plaques in 5XFAD brains (Figure 2). In brain slices obtained from AD patients, astrocytes and microglia have been shown to be associated with the amyloid plaques, where they show an activated, amoeboid state surrounding the plaques with their processes[44,45]. In the case of 5XFAD mice, staining with the astrocytic marker for glial fibrillary acidic protein (GFAP) showed a high number of GFAP-positive cells throughout the subiculum with no colocalization with ferritin positive cells (Figure 3C). However, the selective labeling of microglial cells using tomato lectin, a protein with specific affinity for poly-N-acetyl lactosamine sugar residues that are found on the plasma membrane and in the cytoplasm of microglia, established a high colocalization of this marker with ferritin (Figure 3D). These results indicate that microglial cells colocalized with ferritin and were abundant in areas showing a high density of ferritin and amyloid plaques (Figures 3A and 3B, respectively).

Previous studies suggested that in the brain of patients with AD, the enhanced ferritin expression indicated microglia degeneration instead of reflecting an activated state[45,46]. The enhanced expression of ferritin protein has been described to increase the susceptibility of microglia to degeneration, particularly in the aging brain[45]. Senescent microglia may be less efficient in maintaining iron homeostasis, and free iron could promote oxidative damage in neurodegenerative diseases. Therefore, in brains affected by AD, increased expression of ferritin could constitute a marker of microglial degeneration.

These results indicate that the increased presence of ferritin in AD brains could serve as an interesting biomarker to reveal the presence and localization of amyloid plaques. Therefore, conjugation of an anti-ferritin antibody with magnetic nanoparticles could produce a specific contrast agent useful for noninvasively detecting the presence of amyloid plaques in the brain using MRI.

Coupling of the anti-ferritin antibody to MNPs

An anti-ferritin polyclonal antibody was immobilized onto 50nm dextran-coated MNPs as described in the methods section. A polyclonal antibody that recognizes multiple epitopes on the same antigen was chosen due to its high affinity and tolerance to possible changes in the antigen[47]. The preparation of the nanoconjugates was based on the carbodiimide method[48], leading to the formation of a very stable complex. The efficiency of the antibody binding to the MNPs was determined by a dot-blot assay (Figure 4). Dot-blot analysis confirmed a high level of anti-ferritin antibody binding to MNPs, since only small traces of free anti-ferritin antibody were detected in the unbound fraction (Figure 4C); a high amount of anti-ferritin antibody present at the beginning of the coupling reaction (Figure 4A) could be detected conjugated to the MNPs in the MNPs-anti-ferritin fraction (Figure 4B) after the coupling reaction. Therefore, the binding of the anti-ferritin antibody to the MNPs to form the MNP-anti-ferritin conjugate was highly effective.

These previous results were also confirmed by protein quantification using an improved Bradford protein assay permitting quantification of low protein concentrations[49]. The binding efficiency was estimated to be about 30 ± 14 molecules of anti-ferritin bound per nanoparticle. Binding of the antibody to the MNPs may increase the final hydrodynamic diameter of the MNPs as previously described for similar MNPs[50] in which the antibody bound to the MNPs increased twofold their final hydrodynamic diameter.

Cell viability after incubation with MNPs

To discard a potential neurotoxicity of the MNPs, we determined that the incubation of human neuroblastoma SH-SY5Y cells with MNPs and MNPs-anti-ferritin was feasible and did not impair cell viability in vitro. SH-SY5Y cells were incubated with both types of MNPs and tested for viability using doses up to 200 μg/mL and incubation times of 72 hours, which did not significantly affect neuroblastoma cells survival, as evaluated by the lactate dehydrogenase (LDH) activity assay (Figure 5A). Once determined that MNPs did not induce a loss of cell viability on SHSY5Y cell line, we analyzed the effect of MNP and MNPs-anti-ferritin on primary cell cultures obtained from mouse brains, in order to discard an effect of the MNPs on some specific type of brain cells (i.e.,neurons, astrocytes, or microglial cells). The results showed that cell viability rates were similar in control and MNPs-treated cell cultures (Figure 5B) and that the number of neurons and astrocytes did not decrease in the presence of MNPs or MNPs-anti-ferritin with respect to untreated control cells (Figure 5C). The number of microglia cells stained with the anti-Iba1 antibody were higher in MNPs-treated cells compared to untreated control cells (in which no microglial cells were detected), indicating that MNPs were preferentially taken up by the microglial cells (Figure 5D), although the viability of the cells during the periods of time analyzed was not affected.

These results suggested that although iron oxide nanoparticles could induce oxidative stress[51], the levels of intracellular iron accumulation resulting from the incubation with MNPs and the presence of the antibody in the case of the nanoconjugate MNP-anti-ferritin, did not induce acute cell toxicity at the times and concentrations analyzed. In addition, Mahmoudi and coworkers[52] have shown that the interaction of nanoparticles with serum proteins forming the nanomaterial´s protein corona inhibits the formation of Aβ fibril upon their entrance to the biological medium.

In vitro specificity of the MNP-anti-ferritin conjugate

To verify the in vitro specificity of the MNP-anti-ferritin conjugate, fixed brain sections from 9-month-old 5XFAD and nontransgenic mice, with a high (Figure 6A) and low (Figure 6E) expression of ferritin, respectively, were incubated with the MNP-anti-ferritin conjugate. The

presence of the MNP-anti-ferritin conjugate bound to the subiculum in brain slices was detected using an anti-rabbit-Cy3 antibody which recognized only the polyclonal ferritin antibody bound to the MNPs. The results indicated a strong binding in the case of 5XFAD mice (Figure 6B and 6C) and a nearly absent, undistinguishable from background, binding in nontransgenic mice (Figure 6F and 6G). The accumulation of MNPs in the slices could even be observed by transmission light microscopy as highly localized and crowded black dots in 5XFAD (Figure 6D). This type of signal was undetectable in nontransgenic mice (Figure 6H).

As evidenced in Figure 6, the accumulation of the MNP-anti-ferritin conjugate in the subiculum is higher in 5XFAD than in nontransgenic brain sections (compare Figure 6 B–D with panels F–H). The binding of MNP-anti-ferritin conjugate colocalized with cells showing clear-cut, high expression of ferritin in 5XFAD (Figure 6A) in comparison with nontransgenic (Figure 6E) mice.

Also, the accumulation of bound MNP-anti-ferritin conjugate in the subiculum of 5XFAD mice regionally correlates with the presence of amyloid plaques and ferritin in the subiculum, previously shown in Figure 1D and 1F, respectively. As expected, in brain sections from nontransgenic mice (Figure 6F–H), very few MNP-anti-ferritin nanoconjugate could be detected (Figure 6G), and the black stain observed by transmission light microscopy was absent (Figure 6H), consistent with the very weak expression of ferritin in the subiculum of nontransgenic mice (Figure 6E).

Consequently, these results indicated that the MNP-anti-ferritin conjugate specifically binds and detects the enhanced expression of the ferritin protein that occurs in the subiculum of 9-month-old 5XFAD mice in vitro.

In vivo specificity of the MNP-anti-ferritin conjugate

Once the in vitro specificity of the MNP-anti-ferritin nanoconjugate was confirmed in fixed 5XFAD brain sections, its efficiency was tested in vivo after intravenous injection in 5XFAD mice. Since the previous in vitro results indicated the absence of detectable signal in control

animals, wild type mice were not used in these experiments to reduce the number of animals used in adherence to the 3Rs principles. Plain non-functionalized MNPs and MNP-anti-ferritin conjugates were intravenously injected into the retro-orbital sinus of 5XFAD mice. Six hours after intravenous administration of the MNPs, 5XFAD brains were fixed and subsequently analyzed by histological analyses to localize the final distribution of the MNPs. The accumulation of ferritin protein and amyloid plaques in the subiculum of transgenic mice was again confirmed using an anti-ferritin antibody and Thioflavin-S staining, respectively (Figure 7A). Serial sections were stained with the secondary polyclonal Cy3-antibody alone to detect the presence of the MNP-anti-ferritin conjugates in the subiculum of 5XFAD mice previously injected with the nanoconjugate (Figure 7B). Moreover, the MNPs were fluorescently labeled using an antibody against their coating (antidextran-FITC; Figure 7D and 7G). The results shown in Figure 7 demonstrate that the MNP-antiferritin nanoconjugates injected intravenously accumulate in the subiculum area of the transgenic 5XFAD brains, where a high number of amyloid plaques and an enhanced expression of ferritin exist (Figure 7A–E). In contrast, when non-functionalized MNPs were injected intravenously in 5XFAD mice, only very few, occasional, MNPs could be detected in the subiculum area (Figure 7 F–H), demonstrating a high specificity of the MNP-anti-ferritin conjugates to reveal the accumulation of ferritin in the brain of living 5XFAD mice. These results also indicated that non-functionalized MNPs did not bind to 5XFAD brain parenchyma in a non-specific manner after intravenous injection, demonstrating a lack of nonspecific binding of the non-functionalized MNPs to the iron deposits found in the subiculum of 5XFAD mice. Moreover, the robust colocalization (Figure 7E) of the ferritin antibody signal (Figure 7C) and the MNPs (Figure 7D) indicated that the MNP-anti-ferritin nanoconjugate was highly stable under physiological in vivo conditions, avoiding potential opsonization when circulating through the bloodstream and eluding clearance by the reticuloendothelial system before reaching its target.

The ferritin protein also circulates in the plasma, where it transports iron. Ferritin in plasma has been shown to enter the brain parenchyma through the blood brain barrier (BBB) using the

ferritin H receptor present on the plasma membrane of endothelial cells that form the BBB[53,54]. Therefore, a theoretical drawback of the present method would be that it might be possible that plasmatic ferritin could saturate all the antibody recognition sites available on the MNPs, thus preventing the binding of the nanoconjugate to the ferritin present in the brain parenchyma. This would seriously limit the efficacy of the iron-ferritin detection method, and its potential use as a diagnostic tool. Although we cannot exclude some binding to plasma ferritin, our results indicate that the MNP-anti ferritin conjugate has enough free binding sites to recognize the ferritin accumulated in the subiculum of 5XFAD mice.

Based on our results, we propose that the MNPs conjugated to anti-ferritin antibody could be a useful tool for the imaging and detection of iron accumulations in the brain parenchyma of AD patients. Future work will be needed to increase the binding capacity and affinity of the nanoconjugate. A limitation of our method is the need to open the BBB with the use of mannitol.

Although intravenous mannitol injection has been used safely in patients under a variety of clinical settings[55], a potential future clinical use of this contrast agent would require further modifications including the coupling of MNPs with specific proteins actively transported into the brain[22] or their PEGylation[11] in order to increase the ability of the MNPs to cross the BBB and avoid the use of mannitol.

Ex vivo brain MRI

After confirming that MNP-anti-ferritin nanoconjugate injected intravenously specifically bound to the subiculum region in transgenic 5XFAD brains, MR images from the same area were acquired from a different set of experimental animals after the injection of non-functionalized and functionalized MNPs as a preliminary study. Nontransgenic mice injected with MNP-anti-ferritin and 5XFAD mice without MNPs did not show any non-specific marks in MR images (data not shown). Although there were no evident marks on MR images of the injected MNPs (Figure 8 A and 8B), a significant decrease in T2* value in both the right and

left hippocampus was found in 5XFAD animals injected with functionalized MNPs as compared to 5XFAD mice injected with non-functionalized MNPs (Figure 8 C). Therefore, changes in T2* value in MNP-anti-ferritin injected 5XFAD mice could be attributed to ferritin accumulation and consequently to amyloid plaque deposition in the transgenic mice, as previously demonstrated by histological analysis (Figure 7). Therefore, our results are consistent with the literature. Yang et al[56] also reported a decrease of T2* value in the hippocampus after nanoparticle administration in both in vivo and ex vivo MRI studies.

In order to increase the binding of the nanoconjugate MNPs-anti-ferritin to the transgenic mouse brains, higher amounts of anti-ferritin antibody could be used for the coupling reaction. Moreover, the dosage we used of MNP-anti-ferritin at 20 μmol Fe_3O_4/kg body weight is far from the range of preclinical MRI applications for which contrast agents are typically injected intravenously by femoral or tail vein, at 200 μmol Fe_3O_4/kg body weight for diagnostic purposes[11,29] and similar to the doses of commercial MNPs (i.e., Endorem®, Resovist®, or Feridex®) used in clinical trials (15μmol Fe_3O_4/kg body weight). Therefore, since no cytotoxicity of the MNPs used to synthesize the nanoconjugate was observed even at the highest concentration used (Figure 5), a higher dose of MNPs could be injected in vivo to induce qualitative changes on brain MRI allowing visual ferritin accumulation in the future.

The specificity of this nanoconjugate is important because, to date, the detection of iron deposits associated with AD by MRI is only possible when a high concentration of iron is deposited around the amyloid plaques[12], preventing early diagnosis of the disease. The use of contrast agents like the one described here, based on MNPs functionalized with antibodies directed against the protein that stores iron, would allow an earlier detection of the accumulation of ferritin and, hence, of iron, as we have shown in the present work. This would allow an early diagnosis of the disease, since the presence of iron deposits in the brains of patients with AD is one of the most common histopathological features associated with the disease[17]. Iron is known to promote aggregation of β-amyloid peptide and therefore a large number of therapeutic trials are currently aimed at reducing elevated levels of iron in the brains of AD patients[57]. Thus, an

effective method for early and sensitive detection of iron levels in the brains of AD patients is necessary.

These preliminary results of detecting ferritin accumulation in 5XFAD mice show a potential future high-specificity tool for diagnosis of Alzheimer's disease.

Methods

Animals

Hemizygous 5xFAD mice obtained from the Jackson Laboratory were used as a model of Alzheimer´s disease[37]. These 5xFAD mice carry five mutations associated with familial AD (Swedish (K670N, M671L), Florida (I716V) and London (V717I) mutations in amyloid precursor protein (APP) and M146L and L286V mutations in presenilin 1 (PS1)) and develop several features of AD described in humans, such as the presence of amyloid plaques, which appear as early as 2 months of age in these mice[37]. N=3 Nine month old male 5XFAD transgenic mice and n= 3 their wild-type (nontransgenic) littermates were used for all experiments as proof of concept to determine the specificity of the nanoconjugate. All procedures involving the use of animals were reviewed and approved by the local Animal Care Committee (Universidad Politécnica de Madrid) according to the guidelines of the European Community (ECC/566/2015).

Histological analysis

5XFAD and nontransgenic mice (9-month old) were anesthetized with an overdose of chloral hydrate and intracardially perfused with freshly prepared 4% paraformaldehyde (in 0.1 M phosphate buffer, pH 7.4). Brains were removed, postfixed for 12 h in the same fixative at 4 °C, and dehydrated in 30% sucrose solution at 4 °C until sunk. Thirty-μm thick coronal sections were collected using a freezing microtome (Leica SM 2400).

Prussian blue iron staining was used to visualize the iron deposits in the brain sections of 5XFAD and nontransgenic mice[58]. A previous inactivation of endogenous peroxidase activity in

the tissue was performed by incubating the sections in 3% H_2O_2 and 10% methanol in phosphate buffered saline (PBS); samples were maintained at room temperature in the dark with shaking for 30 minutes. After rinsing with PBS, sections were incubated in the Prussian blue solution (2% potassium ferrocyanide trihydrate (Sigma # P-3289), 2% HCl, 1% Triton X-100 in distilled H_2O) for 30 minutes. Samples were then washed twice in distilled H_2O and treated with a solution of Ni-DAB (5mg of 3, 3'-diaminobenzidine (Sigma), 35 μL of 8% $NiCl_2$ and 4 μL of 30% H_2O_2 in 10 mL of PBS) for 15 minutes. Sections were rinsed in PBS and mounted onto gelatinized glass slides (Menzel-Glaser). The slides were dried overnight, successively dehydrated with ethanol, delipidated with xylene and coverslipped with DPX mounting medium.

Thioflavin S was used for the specific staining of amyloid plaques in brain sections from 5XFAD mice[49,59]. Brain sections from 5XFAD and nontransgenic mice were mounted onto polylysine- treated slides (Thermo Scientific) and allowed to dry for 48h. Sections were then incubated in 0.05% Thioflavin-S (Sigma) diluted in 50% ethanol for 30 minutes, protected from light. After the incubation, sections were rinsed twice in 50% ethanol and once in distilled H_2O. The slides were dried overnight and coverslipped with Mowiol mounting medium.

Immunohistochemistry

Thirty-μm serial sections obtained from 5XFAD and nontransgenic mice were also assessed by immunohistochemistry using a polyclonal antibody against ferritin (1:1000; Sigma) and a monoclonal antibody against GFAP (1:1000; Sternberger). Briefly, free-floating sections were incubated overnight at 4 °C with the primary antibodies diluted in PBS with 2% nonspecific serum. Sections were rinsed four times in PBS for a total time of 1 h and then incubated for 2 h with the secondary antibodies diluted in PBS (anti-mouse or anti-rabbit Cy3- conjugated antibodies, 1:200, all from Jackson Immunoresearch). Streptavidin-FITC (1:300; Vector Labs) was used to detect biotinylated Lectin (1:500; Sigma) for microglial cell staining. Brain sections were mounted onto gelatinized glass slides (Menzel-Glaser). The slides were dried overnight and coverslipped with Mowiol.

Preparation of MNP-anti-ferritin nanoconjugate

MNP-anti-ferritin conjugates were prepared according to the carbodiimide method[48]. Briefly, 1 mg of 50nm in diameter Fe_3O_4-dextran coated MNPs with a magnetite content of 35% (w/w) and functionalized with -COOH groups (Kisker # PMC-50) were washed with 0.1 M 2-(*N*-morpholino)ethanesulfonic acid (MES) buffer at pH 5.5 and diluted to a final volume of 500 μL in MES buffer containing 20 mg of freshly prepared 1-ethyl-3-(3-dimethylaminopropyl) carbodiimide (EDC) and 40 mg of sulfo-*N*-hydroxysuccinimide (NHS). The particles were mixed on a shaker for 2 h at room temperature. After incubation, the particles were washed twice with 1 mL MES buffer at pH 5.5 and the activated particles were resuspended in 0.5 mL MES buffer at pH 5.5. Amine group-containing ligands (150 μg of a polyclonal anti-ferritin human antibody. Sigma-Aldrich Cat. No. F5012) were added to the activated particles and the suspension was mixed on a shaker overnight at room temperature. The conjugate was washed three times with 1 mL PBS, centrifuged each time at 5000 rpm for 5 minutes, resuspended in 0.5 mL of PBS, and kept at 4 ºC until use.

Dot-blot assay

To test the efficiency of the coupling reaction of the anti-ferritin antibody to the MNPs, 1 μL drops of each solution used in the preparation of the MNP-anti-ferritin conjugate (anti-ferritin antibody, MNPs alone, medium containing unbound anti-ferritin antibody, and MNP-anti-ferritin conjugate) were deposited onto a nitrocellulose membrane strip (Bio-Rad). After drying at room temperature, dot-blots were blocked for 1hour at room temperature with 5% skim milk in Tris-buffered saline (500 mM NaCl in 20 mM Tris, pH 7.4) containing 0.05% Tween 20 (TTBS) and then incubated with a goat anti-rabbit peroxidase-conjugated antibody (1:5000; Life Technologies) for 1hour at room temperature. Immunoreactivity was detected using the ECL Western blotting detection system (Amersham Biosciences). In addition, protein concentrations in the coupling reaction (total and unbound antibody) were determined by an improved Bradford protein assay permitting quantification of low protein concentrations[60], in order to confirm dot-blot results. The number of anti-ferritin molecules was calculated as previously

described[61]. In both assays, a control was performed to discard the precipitation of the antibody during the coupling reaction.

Cell viability assays

Human neuroblastoma cells (SH-SY5Y; ECACC No. 94030304) were maintained in DMEM medium supplemented with 10% heat-inactivated fetal bovine serum, 2mM L-glutamine, 0.1mM nonessential amino acids, 100U/mL penicillin and 100 mg/mL streptomycin (Life Technologies). The cell line was maintained at 37ºC in a humidified incubator of 5% CO_2: 95% air and passaged twice per week. For the cell viability assay, cells were plated on 96 well plates ($15x10^3$ cells/well, in triplicate for each condition). Twenty four hours after plating, the cells underwent treatment with MNPs and MNPs-anti-ferritin. Cell viability was evaluated 72 hours after the incubation with the MNPs by the LDH assay, using the Cytotoxicity Detection kit (Roche) and following the manufacturer's instructions. Briefly, after the incubation time with the MNPs, cells were rinsed in PBS and lysed with 1% Triton X-100. Lysate was then collected after centrifugation at 1500 rpm for 5 minutes to remove cell debris. Cell-free supernatants were incubated with the kit´s substrate mixture. LDH activity was determined in a coupled enzymatic reaction; during this reaction, the tetrazolium salt is reduced to formazan. The formazan dye was quantified spectrophotometrically at 490 nm. LDH activity present in the medium was expressed as a percentage of the maximum activity, considering 100% of LDH activity released to the medium as the absorbance obtained when control cells (cells without MNPs) were lysed with 1% Triton X-100.

Cortical mixed neuronal and glial cell cultures were prepared from 18-day-old BCL56 embryos as previously described[62]. Cerebral cortices were enzymatically dissociated in PBS containing 1% bovine serum albumin, 0.4 mg/ml papain, and 6 mM glucose. Dissociated cells were collected by centrifugation (800 x g, 5 minutes) and resuspended in medium supplemented with 20% horse serum. Culture medium consisted of Neurobasal with 1% glutamax-I and B27 supplements (all from Gibco). The cells were then plated at $1x10^5$ cells/cm^2 on plastic plates pretreated for 1 day with 10 mM poly-L-lysine and for 2 hours with laminin (1 mg/ml). The

medium was replaced after 1 day by Neurobasal with 1% glutamax-I and B27 supplements. Two-thirds of the medium were replaced every second day. Cell cultures were maintained for 7 days and then MNPs and MNPs-anti-ferritin were added at 200μg/mL for 3 days. To visualize the final location of MNPs in cortical cell cultures, red fluorescent MNPs (Chemicell nano-screenMAG/R) were used (Figure 5D). Cells were then fixed in 4% paraformaldehyde and immunofluorescence was performed using the following primary antibodies: anti-β-III-tubulin (Sigma) to stain neurons, anti-GFAP (Sigma) to stain astrocytes, and anti-Iba-1 (Sigma) to label microglial cells. Cell nuclei were counterstained with Hoechst 33258 (Molecular Probes). For the cell viability assay, cells were plated on 96-well plates (15×10^3 cells/well, in triplicate for each condition). Twenty-four hours after plating, the cells underwent treatment with MNPs and MNPs-anti-ferritin. Cell viability was evaluated 72 hours after the incubation with the MNPs by using the Cell Proliferation Assay kit (AppliChem) following manufacturer instructions. This employs 2,3-bis-(2-methoxy-4-nitro-5-sulfophenyl)-2H-tetrazolium-5-carboxanilide salt (XTT). In living cells, mitochondria have the capability to reduce XTT to form an orange-colored, water-soluble dye[63]. Therefore, the concentration of this dye is proportional to the number of metabolically active cells. The absorbance of each well was measured spectrophotometrically at 450 nm by using an ELX808 microplate reader (BioTeK).

In vitro specificity of the MNP-anti-ferritin conjugate

To test the specificity of MNP-anti-ferritin conjugates, 5XFAD and nontransgenic brain sections were incubated with the MNP-anti-ferritin nanoconjugate (2 mg/mL). Sections were then washed three times in PBS and incubated for 1hour at room temperature with a goat anti rabbit Cy3 antibody (1:200; Jackson Immunoresearch). Sections were then washed in PBS and distilled water and mounted onto polylysine coated slides (Menzel-Glaser). The slides were dried overnight and coverslipped with Mowiol.

In vivo specificity of the MNP-anti-ferritin conjugate

Mice were anesthetized with a mixture of isoflurane and oxygen (1.5% isoflurane per 1 L oxygen) and homeothermy was maintained through a heated water blanket (TP 500 model, Gaymar Industries, Inc, NY, USA) set at 37 ºC. To facilitate the penetration of the MNPs through the BBB, 100 μL of a solution of mannitol (15% in PBS; Sigma) was injected into the retro-orbital sinus. Then, 15 minutes later, 150 μL (2 mg/mL) of plain MNPs or MNP anti-ferritin conjugate were intravenously injected (approximately 200μg MNPs/mL blood) in the same location[64]. Six hours after injection of the MNPs, mice were intracardially perfused and the brains were fixed as described in the histological analysis section. To identify the presence of the MNP-anti-ferritin nanoconjugate, brain sections were incubated with a secondary anti-rabbit Cy3 antibody (1:200; Jackson Immunoresearch). A monoclonal anti-dextran antibody (1:500; Stem Cell Technologies) and a secondary anti-mouse FITC antibody (1:200; Jackson Immunoresearch) were used to identify the magnetic nanoparticles.

Ex vivo brain MRI

Transgenic 5XFAD mice were injected with MNPs and MNP-anti-ferritin as described in the previous section. Six hours after the injection, mice were transcardially perfused with PBS followed by 4% PFA. After this process, brains were extracted and immersed in Fomblin (Solvay Solexis Inc., Thorofare, NJ) in order to provide a completely dark background around the brains being imaged. A Bruker 7T scanner Biospec 70/20 was used to perform Multiplegradient echo 3D images with the following parameters: 98μm isotropic spatial resolution, TR = 200 ms, matrix =128 × 128 × 128, 10 echoes times (TE), first = 2.7 ms with echo spacing (ES) = 3.57 ms, FA =15°, imaging time = 5hours and 7minutes.

The apparent transverse relaxation time T2* was measured using the ten-echo train image sets described above in several brain regions defined by region of interest (ROI). Right and left dorsal hippocampus were manually drawn and T2* values were obtained using the quantification tool of ParaVision 5.0 (Bruker, Germany).

Optical microscopy

Analyses and photography of Prussian blue or fluorescence stained samples were carried out using an inverted Leica DMIRB microscope equipped with a digital camera (Leica DC100, Nussloch, Germany). The confocal microscopy analysis was performed using a LSM 510 META confocal microscope coupled to an inverted microscope Axiovert200 (Zeiss) with image capture software Zeiss ZEN 2008 sp2.

Statistical analysis

Results are presented as mean ± S.E.M. of at least 3 independent experiments. The data were analyzed by single factor analysis of variance followed by the post hoc Tukey´s honestly significant difference test. A significance level of $p < 0.05$ was chosen. STATISTICA software (StatSoft, Tulsa, OK) was utilized for all statistical tests.

Safety

Not applicable

Abbreviations

AD: Alzheimer´s disease

PET: positron emission tomography

MNPs: magnetic iron oxide nanoparticles

MRI: magnetic resonance imaging

5XFAD: transgenic mice model with five familial Alzheimer's disease mutations

PBS: phosphate buffered saline

GFAP: glial fibrillary acidic protein

LDH: lactate dehydrogenase

MES: 2-(N-morpholino) ethanesulfonic acid

BBB: blood brain barrier

DDNP: 1,1-dicyano-2-[6-(dimethylamino)naphthalene-2-yl] propene

Author Information

*Corresponding autor

Milagros Ramos-Gómez*

Centre for Biomedical Technology (CTB), Universidad Politécnica de Madrid. Campus de Montegancedo, Pozuelo de Alarcón, 28223 Madrid, Spain

*E-mail: milagros.ramos@ctb.upm.es

Author Contributions

MRG and AMS conceived the study, participated in its design and coordination and drafted the manuscript. TFC, LC and MD carried out all experimental studies and helped to draft the manuscript.

Funding Sources

This work was supported by Reina Sofia Foundation (to MRG). This study was also funded by the Comunidad de Madrid (Neurotec-S2010/BMD-2460). Work at AMS laboratory was funded by MINECO (SAF2010-17167 and SAF2014-56101-R), Comunidad de Madrid (Neurostem-CM S2010-BMD-2336) and Instituto de Salud Carlos III (RETIC TerCel, RD12/0019/0013). Work at MD laboratory was cofunded by FEDER "Una manera de hacer Europa" and the Comunidad de Madrid (BRADE S2013/ICE-2958).

Conflict of Interest

The authors declare that they have no competing interests.

Acknowledgment

We would like to thank Beatriz Moreno and Soledad Martinez for the excellent technical assistance. We thank Dr. R. Martínez (Cajal Institute, Madrid, Spain) for providing the Iba1 antibody.

References

(1) (2016) World Alzheimer Report 2016 Improving healthcare for people living with dementia coverage, Quality and costs now and in the future.

(2) Apostolova, L. G., Hwang, K. S., Andrawis, J. P., Green, A. E., Babakchanian, S., Morra, J. H., Cummings, J. L., Toga, A. W., Trojanowski, J. Q., Shaw, L. M., Jack, C. R., Petersen, R. C., Aisen, P. S., Jagust, W. J., Koeppe, R. A., Mathis, C. A., Weiner, M. W., and Thompson, P. M. (2010) 3D PIB and CSF biomarker associations with hippocampal atrophy in ADNI subjects. *Neurobiol. Aging 31*, 1284–1303.

(3) Smailagic, N., M, R. F., Ciapponi, A., Giannakou, A., Ol, P., X, B. C., and Cullum, S. (2015) Mini-Mental State Examination (MMSE) for the detection of Alzheimer ' s disease and other dementias in people with mild cognitive impairment (MCI) (Review). *Cochrane Database Syst Rev* CD010783.

(4) Reiman, E. M., Quiroz, Y. T., Fleisher, A. S., Chen, K., Velez-Pardo, C., Jimenez-Del-Rio, M., Fagan, A. M., Shah, A. R., Alvarez, S., Arbelaez, A., Giraldo, M., Acosta-Baena, N., Sperling, R. A., Dickerson, B., Stern, C. E., Tirado, V., Munoz, C., Reiman, R. A., Huentelman, M. J., Alexander, G. E., Langbaum, J. B. S., Kosik, K. S., Tariot, P. N., and Lopera, F. (2012) Brain imaging and fluid biomarker analysis in young adults at genetic risk for autosomal dominant Alzheimer's disease in the presenilin 1 E280A kindred: A case-control study. *Lancet Neurol. 11*, 1048–1056.

(5) Koffie, R. M., Farrar, C. T., Saidi, L.-J., William, C. M., Hyman, B. T., and Spires-Jones, T. L. (2011) Nanoparticles enhance brain delivery of blood-brain barrier-impermeable probes for in vivo optical and magnetic resonance imaging. *Proc. Natl. Acad. Sci. 108*, 18837–18842.

(6) Chamberlain, R., Wengenack, T. M., Poduslo, J. F., Garwood, M., and Jack, C. R. (2011) Magnetic resonance imaging of amyloid plaques in transgenic mouse models of Alzheimer's disease. *Curr. Med. Imaging Rev. 7*, 3–7.

(7) Baltes, C., Princz-Kranz, F., Rudin, M., and Mueggler, T. (2011) Detecting amyloid-β plaques in Alzheimer's disease. *Methods Mol. Biol. 711*, 511–533.

(8) Wisniewski T, B. A. (2010) Vaccination as a therapeutic approach to Alzheimer's disease. *Mt Sinai J Med 77*, 17–31.

(9) Thomas Wisniewskia, A. E. M. S. (2010) Murine models of Alzheimer's disease and their use in developing immunotherapies. *Biochim Biophys Acta. 1802*, 847–859.

(10) Wadghiri, Y. Z., Sigurdsson, E. M., Sadowski, M., Elliott, J. I., Li, Y., Scholtzova, H., Tang, C. Y., Aguinaldo, G., Pappolla, M., Duff, K., Wisniewski, T., and Turnbull, D. H. (2003) Detection of Alzheimer's amyloid in transgenic mice using magnetic resonance microimaging. *Magn. Reson. Med. 50*, 293–302.

(11) Wadghiri, Y. Z., Li, J., Wang, J., Hoang, D. M., Sun, Y., Xu, H., Tsui, W., Li, Y., Boutajangout, A., Wang, A., de Leon, M., and Wisniewski, T. (2013) Detection of Amyloid Plaques Targeted by Bifunctional USPIO in Alzheimer's Disease Transgenic Mice Using Magnetic Resonance Microimaging. *PLoS One 8*, 1–10.

(12) Wadghiri YZ, Hoang DM, Wisniewski T, S. E. (2012) In vivo magnetic resonance imaging of amyloid-β plaques in mice. *Methods Mol Biol 849*, 435–451.

(13) Benveniste, H., Einstein, G., Kim, K. R., Hulette, C., and Johnson, G. A. (1999) Detection of neuritic plaques in Alzheimer's disease by magnetic resonance microscopy. *Proc. Natl. Acad. Sci. 96*, 14079–14084.

(14) Braakman, N., Matysik, J., Van Duinen, S. G., Verbeek, F., Schliebs, R., de Groot, H. J. M., and Alia, A. (2006) Longitudinal assessment of Alzheimer's beta-amyloid plaque development in transgenic mice monitored by in vivo magnetic resonance microimaging. *J.*

Magn. Reson. Imaging 24, 530–536.

(15) Jack, C. R. (2005) In Vivo Magnetic Resonance Microimaging of Individual Amyloid Plaques in Alzheimer's Transgenic Mice. *J. Neurosci. 25*, 10041–10048.

(16) Vanhoutte, G., Dewachter, I., Borghgraef, P., Van Leuven, F., and Van Der Linden, A. (2005) Noninvasive in vivo MRI detection of neuritic plaques associated with iron in APP[V717I] transgenic mice, a model for Alzheimer's disease. *Magn. Reson. Med. 53*, 607–613.

(17) Connor, J. R., Menzies, S. L., Martin, S. M. S., and Mufson, E. J. (1992) A Histochemical Study of Iron , Transferrin , and Ferritin in Alzheimer ' s Diseased Brains. *J. Neurosci. Res. 83*, 75–83.

(18) Meadowcort, M. D., Connor, J. R., Smith, M. B., and Yang, Q. X. (2009) Magnetic Resonance Imaging and Histological Analysis of Beta- Amyloid Plaques in Both Human Alzheimer's Disease and APP/ PS1 Transgenic Mice. *J Magn Reson Imaging 29*, 997–1007.

(19) Yang, C. C., Yang, S. Y., Chieh, J. J., Horng, H. E., Hong, C. Y., Yang, H. C., Chen, K. H., Shih, B. Y., Chen, T. F., and Chiu, M. J. (2011) Biofunctionalized magnetic nanoparticles for specifically detecting biomarkers of Alzheimer's disease in vitro. *ACS Chem. Neurosci. 2*, 500–505.

(20) McLachlan, S. J., Morris, M. R., Lucas, M. A., Fisco, R. A., Eakins, M. N., Fowler, D. R., Scheetz, R. B., and Olukotun, A. Y. (1994) Phase I clinical evaluation of a new iron oxide MR contrast agent. *J. Magn. Reson. Imaging 4*, 301–307.

(21) Wadghiri YZ, Sigurdsson EM, Wisniewski T, T. D. (2005) MR Imaging of amyloid plaques in transgenic mice, in *Amyloid proteins: Methods and Protocols* (EM, S., Ed.), pp 365–379. Humana Press Inc, Totowa, New Jersey.

(22) Sigurdsson, E. M., Wadghiri, Y. Z., Mosconi, L., Blind, J. A., Knudsen, E., Asuni, A., Scholtzova, H., Tsui, W. H., Li, Y., Sadowski, M., Turnbull, D. H., de Leon, M. J., and

Wisniewski, T. (2008) A non-toxic ligand for voxel-based MRI analysis of plaques in AD transgenic mice. *Neurobiol. Aging 29*, 836–847.

(23) Plissonneau, M., Pansieri, J., Heinrich-Balard, L., Morfin, J.-F., Stransky-Heilkron, N., Rivory, P., Mowat, P., Dumoulin, M., Cohen, R., Allémann, É., Tóth, É., Saraiva, M. J., Louis, C., Tillement, O., Forge, V., Lux, F., and Marquette, C. (2016) Gd-nanoparticles functionalization with specific peptides for ß-amyloid plaques targeting. *J. Nanobiotechnology 14*, 60.

(24) Ansciaux, E., Burtea, C., Laurent, S., Crombez, D., Nonclercq, D., Vander Elst, L., and Muller, R. N. (2015) In vitro and in vivo characterization of several functionalized ultrasmall particles of iron oxide, vectorized against amyloid plaques and potentially able to cross the blood-brain barrier: Toward earlier diagnosis of Alzheimer's disease by molecular imag. *Contrast Media Mol. Imaging 10*, 211–224.

(25) Poduslo JF, Hultman KL, Curran GL, Preboske GM, Chamberlain R, Marjańska M, et al. (2011) Targeting vascular amyloid in arterioles of Alzheimer disease transgenic mice with amyloid β protein antibody-coated nanoparticles. *J Neuropathol Exp Neurol 70*, 653–661.

(26) Jaruszewski, K. M., Curran, G. L., Swaminathan, S. K., Rosenberg, J. T., Grant, S. C., Ramakrishnan, S., Lowe, V. J., Poduslo, J. F., and Kandimalla, K. K. (2014) Multimodal Nanoprobes to target cerebrovascular amyloid in Alzheimer's disease brain. *Biomaterials 35*, 1967–1976.

(27) Yin, Z., Yu, T., and Xu, Y. (2015) Preparation of Amyloid Immuno-Nanoparticles as Potential MRI Contrast Agents for Alzheimer's Disease Diagnosis. *J. Nanosci. Nanotechnol. 15*, 6429–6434.

(28) Siegemund, T., Paulke, B. R., Schmiedel, H., Bordag, N., Hoffmann, A., Harkany, T., Tanila, H., Kacza, J., and Härtig, W. (2006) Thioflavins released from nanoparticles target fibrillar amyloid β in the hippocampus of APP/PS1 transgenic mice. *Int. J. Dev. Neurosci. 24*, 195–201.

(29) Hu, B., Dai, F., Fan, Z., Ma, G., Tang, Q., and Zhang, X. (2015) Nanotheranostics: Congo Red/Rutin-MNPs with Enhanced Magnetic Resonance Imaging and H2 O2 -Responsive Therapy of Alzheimer's Disease in APPswe/PS1dE9 Transgenic Mice. *Adv. Mater.* 27 (37):5499-5505.

(30) Zhang, D., Fa, H.-B., Zhou, J.-T., Li, S., Diao, X.-W., and Yin, W. (2015) The detection of β-amyloid plaques in an Alzheimer's disease rat model with DDNP-SPIO. *Clin. Radiol. 70*, 74–80.

(31) Cheng, K. K., Chan, P. S., Fan, S., Kwan, S. M., Yeung, K. L., Wang, Y. X. J., Chow, A. H. L., Wu, E. X., and Baum, L. (2015) Curcumin-conjugated magnetic nanoparticles for detecting amyloid plaques in Alzheimer's disease mice using magnetic resonance imaging (MRI). *Biomaterials 44*, 155–172.

(32) Altamura, S., and Muckenthaler, M. U. (2009) Iron toxicity in diseases of aging: Alzheimer's disease, Parkinson's disease and atherosclerosis. *J. Alzheimer's Dis. 16*, 879–895.

(33) Bartzokis G, T. T. (2000) MRI evaluation of basal ganglia ferritin iron and neurotoxicity in Alzheimer's and Huntingon's disease. *Cell Mol Biol 46*, 821–833.

(34) Sultana, R., Boyd-Kimball, D., Cai, J., Pierce, W. M., Klein, J. B., Merchant, M., and Butterfield, D. A. (2007) Proteomics analysis of the Alzheimer's disease hippocampal proteome. *J. Alzheimers. Dis. 11*, 153–164.

(35) Rogers JT, Bush AI, Cho HH, Smith DH, Thomson AM, Friedlich AL, Lahiri DK, Leedman PJ, Huang X, C. C. (2008) Iron and the translation of the amyloid precursor protein (APP) and ferritin mRNAs: riboregulation against neural oxidative damage in Alzheimer's disease. *Biochem Soc Trans 36*, 1282–1287.

(36) Grundke-Iqbal, I., Fleming, J., Tung, Y. C., Lassmann, H., Iqbal, K., and Joshi, J. G. (1990) Ferritin is a component of the neuritic (senile) plaque in Alzheimer dementia. *Acta Neuropathol. 81*, 105–110.

(37) Oakley, H., Cole, S. L., Logan, S., Maus, E., Shao, P., Craft, J., Guillozet-Bongaarts, A., Ohno, M., Disterhoft, J., Van Eldik, L., Berry, R., and Vassar, R. (2006) Intraneuronal β-Amyloid Aggregates, Neurodegeneration, and Neuron Loss in Transgenic Mice with Five Familial Alzheimer's Disease Mutations: Potential Factors in Amyloid Plaque Formation. *J. Neurosci. 26*, 10129–10140.

(38) Smith, M. A., Harris, P. L., Sayre, L. M., and Perry, G. (1997) Iron accumulation in Alzheimer disease is a source of redox-generated free radicals. *Proc. Natl. Acad. Sci. U. S. A. 94*, 9866–9868.

(39) Abo-Krysha, N., and Rashed, L. (2008) The role of iron dysregulation in the pathogenesis of multiple sclerosis: an Egyptian study. *Mult. Scler. 14*, 602–608.

(40) Raven, E. P., Lu, P. H., Tishler, T. A., Heydari, P., and Bartzokis, G. (2013) Increased iron levels and decreased tissue integrity in hippocampus of Alzheimer's disease detected in vivo with magnetic resonance imaging. *J. Alzheimer's Dis. 37*, 127–136.

(41) Chen, J., Marks, E., Lai, B., Zhang, Z., Duce, J. A., Lam, L. Q., Volitakis, I., Bush, A. I., Hersch, S., and Fox, J. H. (2013) Iron Accumulates in Huntington's Disease Neurons: Protection by Deferoxamine. *PLoS One 8*, 1–12.

(42) Mochizuki, H., and Yasuda, T. (2012) Iron accumulation in Parkinson's disease. *J. Neural Transm. 119*, 1511–1514.

(43) Hametner, S., Wimmer, I., Haider, L., Pfeifenbring, S., Brück, W., and Lassmann, H. (2013) Iron and neurodegeneration in the multiple sclerosis brain. *Ann. Neurol. 74*, 848–861.

(44) Meadowcroft, M. D., Connor, J. R., and Yang, Q. X. (2015) Cortical iron regulation and inflammatory response in Alzheimer's disease and APP SWE/PS1ΔE9 mice: A histological perspective. *Front. Neurosci. 9*, 1–16.

(45) Lopes, K. O., Sparks, D. L., and Streit, W. J. (2008) Microglial dystrophy in the aged and Alzheimer's disease brain is associated with ferritin immunoreactivity. *Glia 56*, 1048–1060.

(46) Mrak, R.E. (2012) Microglia in Alzheimer brain: a neuropathological perspective. *Int J Alzheimers Dis 2012*, 165021.

(47) Lipman, N. S., Jackson, L. R., Weis-Garcia, F., and Trudel, L. J. (2005) Monoclonal versus polyclonal antibodies: distinguishing characteristics, applications, and information resources. *ILAR J. 46*, 258–268.

(48) Monagle, J. J. (1962) Carbodiimides. III. Conversion of isocyanates to carbodiimides-catalyst studies. *J. Org. Chem. 27*, 3851–3855.

(49) Schmidt, M. L., Robinson, K. A., Lee, V. M., and Trojanowski, J. Q. (1995) Chemical and immunological heterogeneity of fibrillar amyloid in plaques of Alzheimer's disease and Down's syndrome brains revealed by confocal microscopy. *Am. J. Pathol. 147*, 503–515.

(50) Mu, K., Zhang, S., Ai, T., Jiang, J., Yao, Y., Jiang, L., Zhou, Q., Xiang, H., Zhu, Y., Yang, X., and Zhu, W. (2015) Monoclonal antibody-conjugated superparamagnetic iron oxide nanoparticles for imaging of epidermal growth factor receptor-targeted cells and gliomas. *Mol. Imaging 14*.

(51) Novotna, B., Jendelova, P., Kapcalova, M., Rossner, P., Turnovcova, K., Bagryantseva, Y., Babic, M., Horak, D., and Sykova, E. (2012) Oxidative damage to biological macromolecules in human bone marrow mesenchymal stromal cells labeled with various types of iron oxide nanoparticles. *Toxicol. Lett. 210*, 53–63.

(52) Mahmoudi, M., Monopoli, M. P., Rezaei, M., Lynch, I., Bertoli, F., Mcmanus, J. J., and Dawson, K. A. (2013) The Protein Corona Mediates the Impact of Nanomaterials and Slows Amyloid Beta Fibrillation. *ChemBioChem 14*, 568–572.

(53) Li, L., Fang, C. J., Ryan, J. C., Niemi, E. C., Lebrón, J. a, Björkman, P. J., Arase, H., Torti, F. M., Torti, S. V, Nakamura, M. C., and Seaman, W. E. (2010) Binding and uptake of H-ferritin are mediated by human transferrin receptor-1. *Proc. Natl. Acad. Sci. U. S. A. 107*, 3505–3510.

(54) Wallace, D. F., McDonald, C., and Subramaniam, V. N. (2010) Transferrin receptor 1: A ferritin receptor as well? *Gastroenterology 139*, 1052–1053.

(55) Brown, R. C., Egleton, R. D., and Davis, T. P. (2004) Mannitol opening of the blood-brain barrier: Regional variation in the permeability of sucrose, but not 86Rb+ or albumin. *Brain Res. 1014*, 221–227.

(56) Jing Yang, Youssef Zaim Wadghiri, Dung Minh Hoang, Wai Tsui, Yanjie Sun, E., and Chung, Yongsheng Li, Andrew Wang, M. de L. and T. W. (2011) Detection of Amyloid Plaques Targeted by USPIO-Aβ1-42 in Alzheimer's Disease Transgenic Mice using Magnetic Resonance Microimaging. *Neuroimage 55*, 1600–1609.

(57) Bush, A. I., and Tanzi, R. E. (2008) Therapeutics for Alzheimer's disease based on the metal hypothesis. *Neurotherapeutics 5*, 421–432.

(58) Hall, a P., Davies, W., Stamp, K., Clamp, I., and Bigley, A. (2013) Comparison of Computerized Image Analysis with Traditional Semiquantitative Scoring of Perls' Prussian Blue Stained Hepatic Iron Deposition. *Toxicol. Pathol.* 992–1000.

(59) Bussière, T., Bard, F., Barbour, R., Grajeda, H., Guido, T., Khan, K., Schenk, D., Games, D., Seubert, P., and Buttini, M. (2004) Morphological characterization of Thioflavin-S-positive amyloid plaques in transgenic Alzheimer mice and effect of passive Abeta immunotherapy on their clearance. *Am. J. Pathol. 165*, 987–995.

(60) Ernst, O., and Zor, T. (2010) Linearization of the Bradford Protein Assay. *J. Vis. Exp.* 1–6.

(61) Fernández-Cabada, T., Pablo, C. S.-L. de, Pisarchyk, L., Serrano-Olmedo, J. J., and Ramos-Gómez, M. (2016) Optical Hyperthermia Using Anti-Epidermal Growth Factor Receptor-Conjugated Gold Nanorods to Induce Cell Death in Glioblastoma Cell Lines. *J. Nanosci. Nanotechnol. 16*, 7689–7695.

(62) Alvarez, G., Muñoz-Montaño, J. R., Satrústegui, J., Avila, J., Bogónez, E., Díaz-Nido, J., and Díaz-Nido, J. (1999) Lithium protects cultured neurons against beta-amyloid-induced

neurodegeneration. *FEBS Lett. 453*, 260–264.

(63) Berridge, M. V., Herst, P. M., and Tan, A. S. (2005) Tetrazolium dyes as tools in cell biology: New insights into their cellular reduction. *Biotechnol. Annu. Rev. 11,* 127-152.

(64) Yardeni, T., Eckhaus, M., Morris, H. D., Huizing, M., and Hoogstraten-Miller, S. (2011) Retro-orbital injections in mice. *Lab Anim. (NY). 40*, 155–160.

Figure captions

Figure 1: **Iron, amyloid, and ferritin accumulation in 5XFAD mice.** Coronal brain sections of nontransgenic (**A, C,** and **E**) and 5XFAD transgenic (**B, D,** and **F**) mice stained with: **A** and **B)** Prussian blue to detect iron accumulation; **C** and **D)** Thioflavin S to label amyloid plaques; and **E** and **F)** an anti-ferritin antibody to detect the protein ferritin. No obvious label of any markers can be detected in nontransgenic mice, while the subiculum in 5XFAD mice showed a strong labeling for iron (arrow in **B**), amyloid plaques (arrow in **D**), and ferritin (arrow in **F**). Scale bars in **A** and **B**: 200 μm and in **C-F**: 500 μm.

Figure 2: Spatial relationship between ferritin and amyloid plaques in 5XFAD mice. Serial confocal microscopy images obtained every 5 μm from the top of the section to the bottom (**A through D**) in the Z axis from the subiculum of a 5XFAD mouse. Coronal brain sections were labeled with an antibody anti-ferritin (red) and Thioflavin S (green) to detect the presence of ferritin and amyloid plaques, respectively. Scale bar: 25 μm.

Figure 3: Cell types that accumulate ferritin in 5XFAD mice. A) Coronal brain section of a 5XFAD mouse stained with an anti-ferritin antibody showing the accumulation of ferritin in the subiculum area (arrow). **B)** Higher magnification of the same anatomical region showing a high regional colocalization of amyloid plaques stained with Thioflavin S (green) and the anti-ferritin antibody (red). **C)** Sections stained with the astrocytic marker GFAP (green) showed a high number of GFAP-positive cells throughout the subiculum area with no colocalization with the ferritin-positive cells (red). **D)** Microglial cells in the subiculum area labeled with tomato lectin

(green) showing a high degree of colocalization (yellow) with the ferritin stain (anti-ferritin antibody in red). Scale bars in **A**: 500 μm; in **B-D**: 100 μm.

Figure 4: Dot-blot assay to determine the effectiveness of the anti-ferritin antibody coupling to MNPs. One μl of **A)** anti-ferritin antibody used for the coupling reaction, **B)** MNPs functionalized with the anti-ferritin antibody, **C)** supernatant after the coupling reaction (anti-ferritin antibody not bound to MNPs), and **D)** MNPs used as a negative control. Note that a very high fraction of the initial antibody present in the coupling reaction did bind to the MNPs.

Figure 5: Cell viability after incubation with magnetic nanoparticles. Analysis of the viability of human neuroblastoma SH-SY5Y cells (**A**) and neuronal-glia mixed primary cell cultures obtained from mouse brains (**B**) exposed to increasing concentrations of MNPs and MNP-anti-ferritin for 72 hours, assessed by the LDH and XTT assays, respectively. No remarkable changes in cell viability were observed when cells were exposed to increasing concentrations of both types of MNPs for 72 hours. Cell viability in LDH and XTT assays was considered maximum (100%) when cells were incubated without MNPs. The number of neurons, astrocytes and microglial cells did not show any changes when primary cell cultures obtained from mouse brains were incubated with either MNPs or MNPs-anti-ferritin (**C**). Microfluorescence images of red fluorescent MNPs-treated cell cultures stained with anti-β-III-tubulin (neurons), anti-GFAP (astrocytes) and anti-Iba1 (microglia) in green show that the nanoparticles are uptaken preferentially by microglial cells (D). Inserts in D show single staining for fluorescent MNPs (red) and microglial cells stained with anti-Iba-1 (green). Nuclei were counterstained with Hoechst (blue). Each value in the graph bars represents the mean ± SEM of n = 3 independent experiments. ANOVA followed by the post-hoc Tukey´s test revealed the absence of significant differences ($p>0.05$) for each group compared to untreated cells with MNPs. Scale bar in **D**: 50μm.

Figure 6: *In vitro* specificity of the MNP-anti-ferritin conjugate. Coronal brain sections of 5XFAD (**A**) and nontransgenic (**E**) mice were stained with an antibody anti-ferritin to determine

the accumulation of this protein in the subiculum region (boxes in **A** and **E**). Note the high accumulation of ferritin in 5XFAD brain compared to nontransgenic mice. Coronal brain sections of 5XFAD (**B-D**) and nontransgenic (**F-H**) mice, adjacent to those shown in **A** and **E** respectively, were incubated first with the nanoconjugate MNP-anti-ferritin and then with a secondary antibody-Cy3 to detect the presence of the nanoconjugate MNP-anti-ferritin stained in red (**C, G**). MNPs were also detected by transmitted light microscopy as black dots in 5XFAD (**D**) and nontransgenic (**H**) mice. **B** and **F** show merged images of **C** and **D**, and **G** and **H**, respectively. Note the high rate of colocalization of ferritin and MNPs (**B**) demonstrating an optimal biofunctionalization of the particles and the absence of binding of the nanoconjugate to the nontransgenic brain sections (**F-H**) where no ferritin accumulation can be detected (**E**). Scale bars: **A** and **E**: 500 μm; **B-D** and **F-H**: 50 μm.

Figure 7: *In vivo* specificity of the MNP-anti-ferritin conjugate in 5XFAD mice. Coronal brain section of a 5XFAD mouse showing **A**) the accumulation of ferritin (red) and amyloid plaques stained with Thioflavin S (green); **B**) the subiculum region of a 5XFAD mouse previously injected intravenously with the MNP-anti-ferritin conjugate, showing the presence of the MNP-anti-ferritin nanoconjugate (red) closely bound to amyloid plaques stained with Thioflavin S (green). Coronal sections of the subiculum of 5XFAD mice injected with the functionalized MNP-anti-ferritin nanoconjugate (**C**-**E**) and with the non-functionalized MNPs (**F**-**H**). The anti-ferritin antibody of the nanoconjugate was detected using a secondary antibody-Cy3 (red) (**C**, **F**). All MNPs were detected using an anti-dextran-FITC antibody (green) (**D**, **G**). Merged images of **C** and **D**, and **F** and **G** are shown in **E** and **H**, respectively. Note the high accumulation of MNPs in the subiculum of animals injected with the nanoconjugate MNP-anti-ferritin (**C-E**) and the absence of MNPs in the same area when non-functionalized MNPs were used (**F-H**). Scale bars: **A** and **B**: 100 μm; **C**-**H**: 50 μm.

Figure 8: *Ex vivo* MRI in 5XFAD mice. Ex vivo MR images used to determine absolute T2* values (msec) in regions of interest (ROIs), which were the left and right hippocampus of 5XFAD mice injected with MNPs (A) and MNPs-anti-ferritin (B). Graphic shows the data

corresponding to the T2* value obtained in the analyzed ROIs of the left and right hippocampus in 5XFAD mice injected with MNPs versus MNP-anti-ferritin (*$p < 0.05$; ANOVA followed by the post-hoc Tukey´s test).

Potential use of the MNP-anti-ferritin nanoconjugate as an effective MRI contrast agent for the diagnosis of Alzheimer´s disease

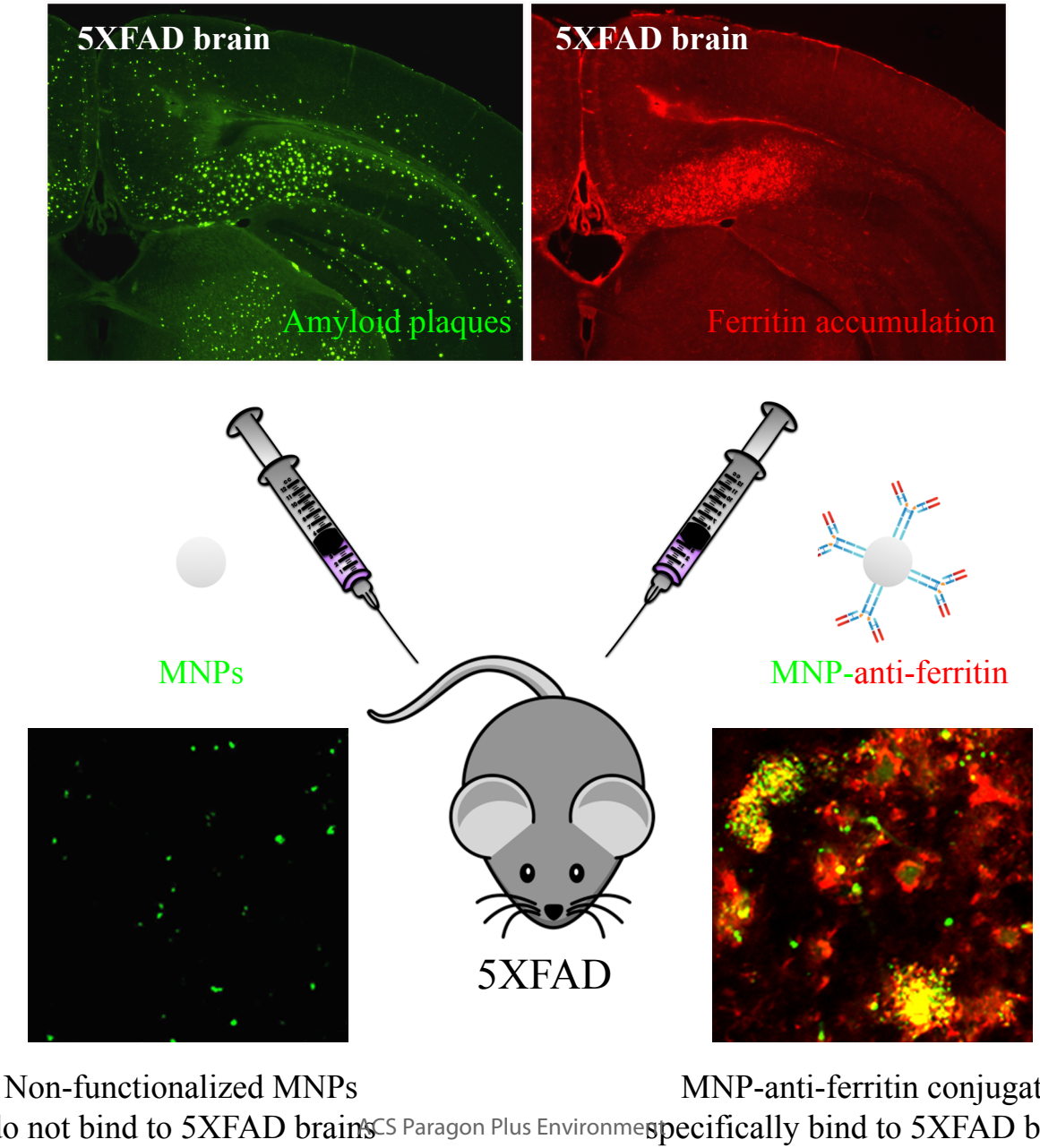

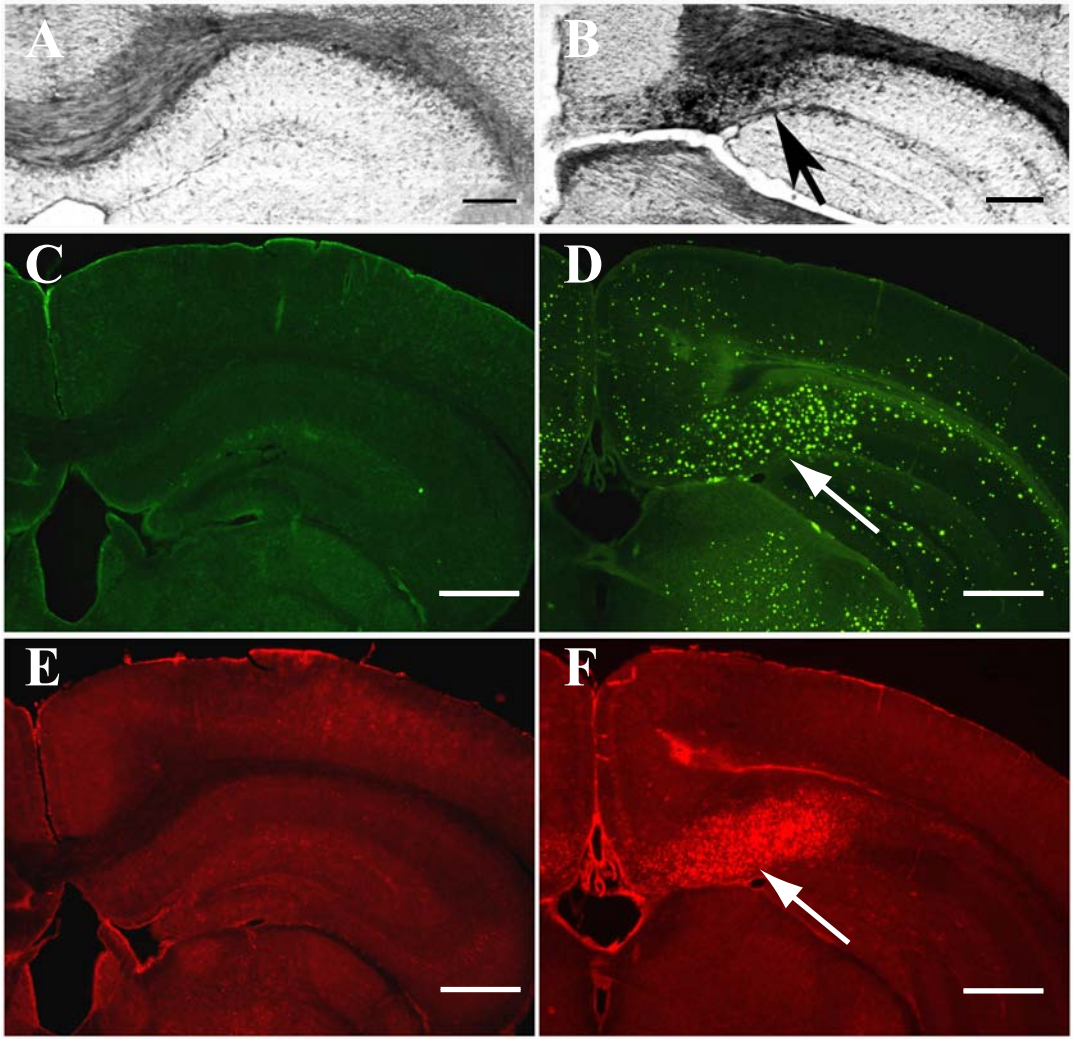

Figure 1

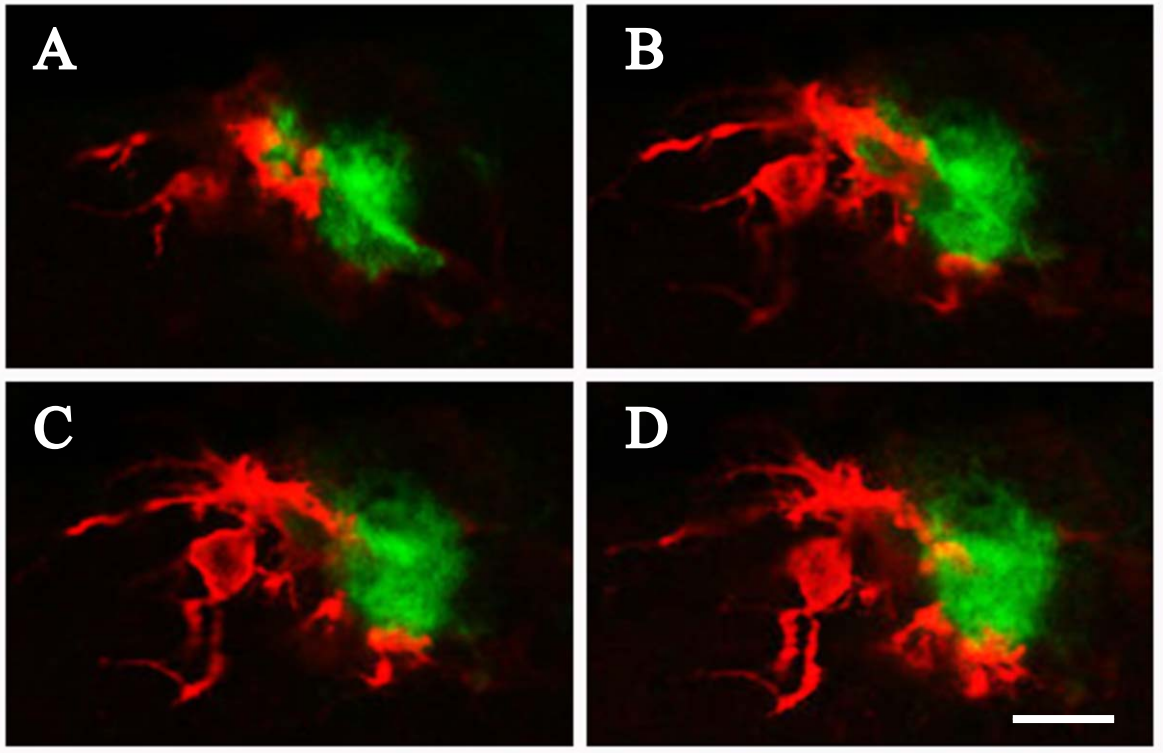

Figure 2

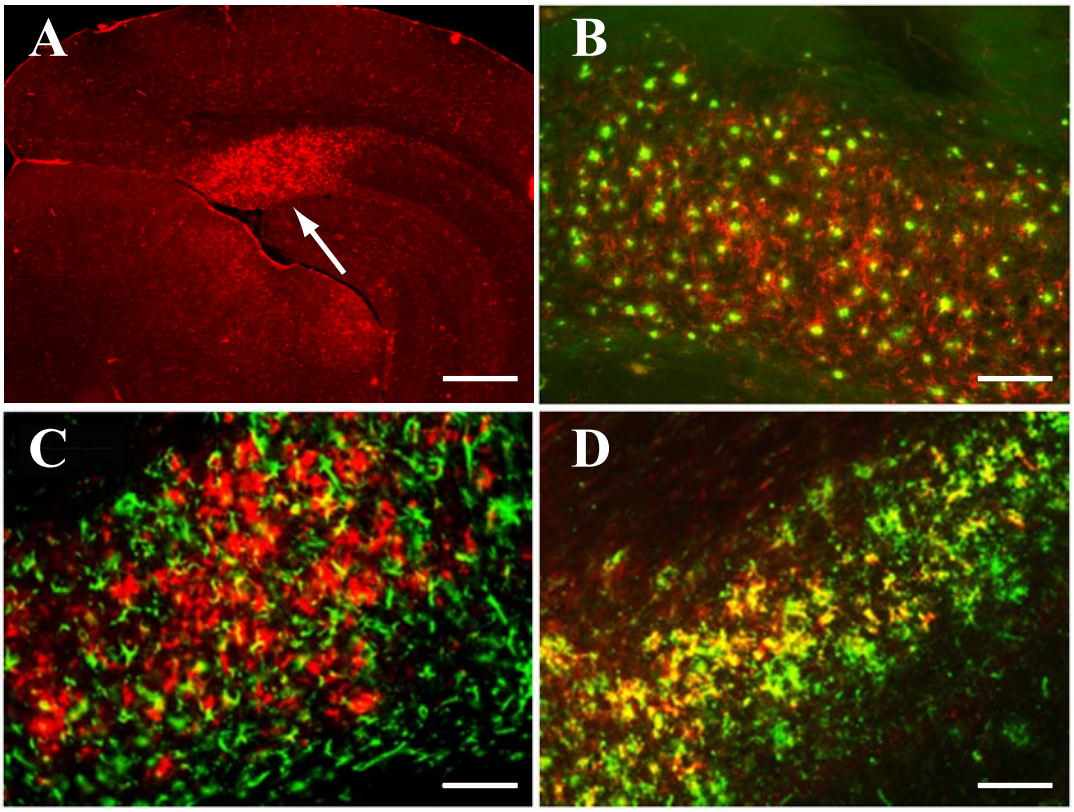

Figure 3

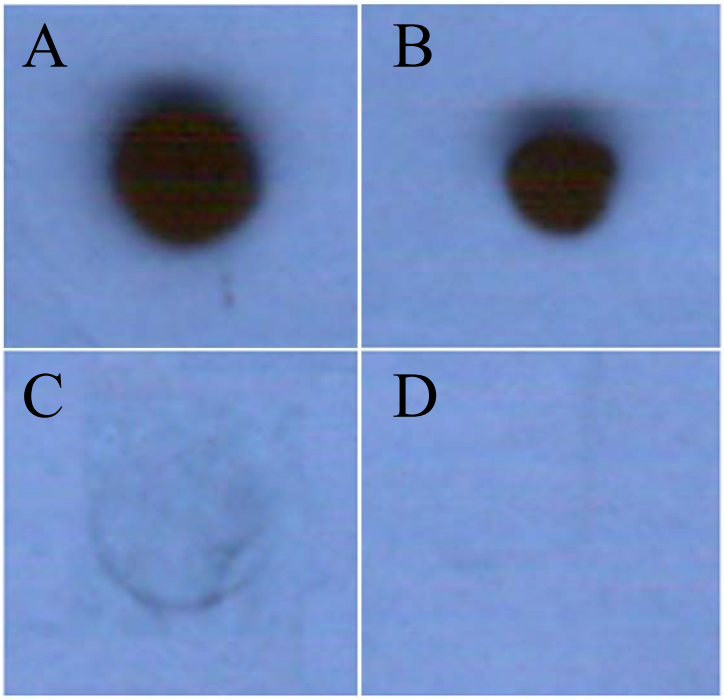

Figure 4

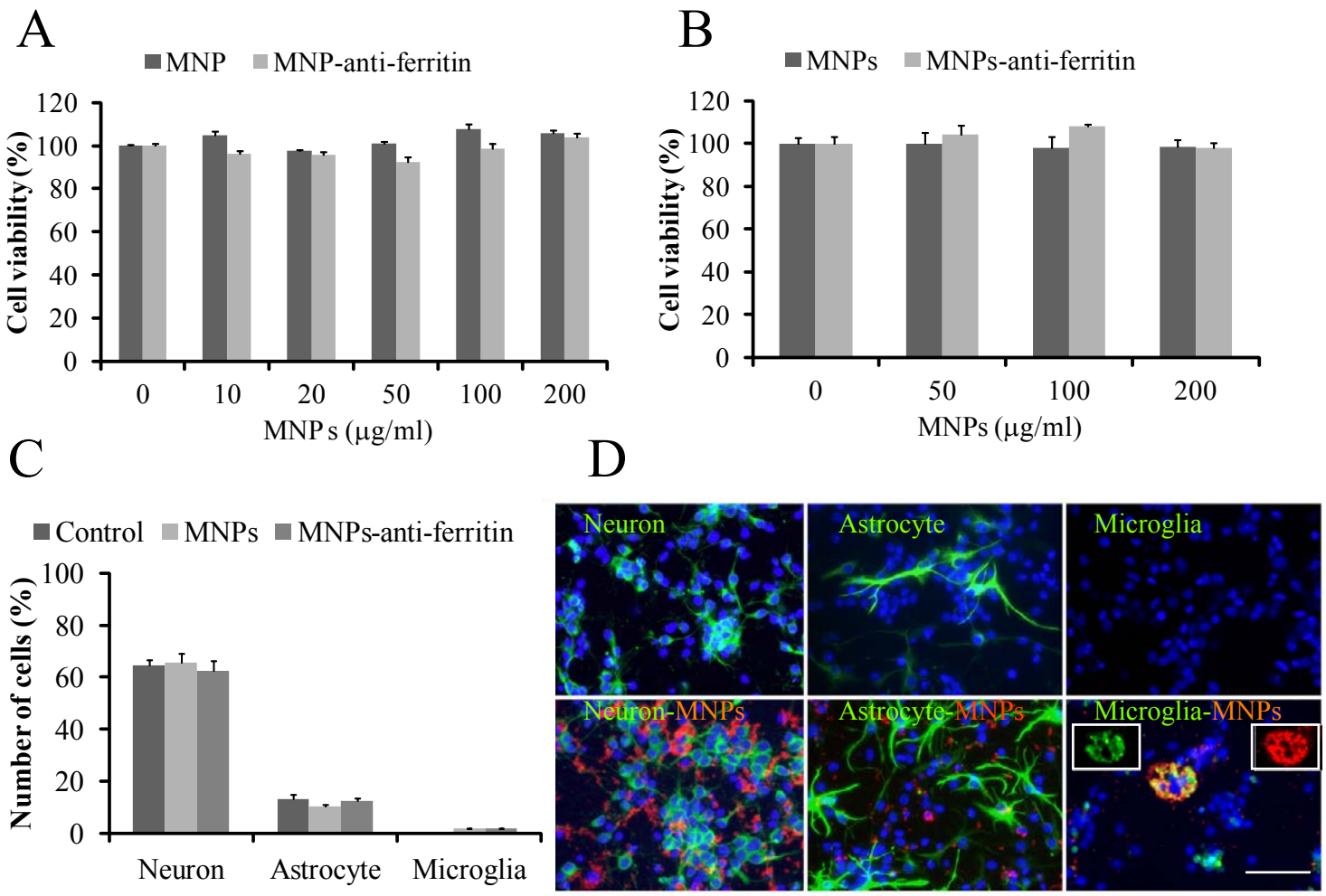
A
MNP
MNP-anti-ferritin
Cell viability (%)
120
100
80
60
40
20
0
0
10
20
50
100
200
MNP s (μg/ml)
B
MNPs
MNPs-anti-ferritin
Cell viability (%)
120
100
80
60
40
20
0
0
50
100
200
MNPs (μg/ml)
C
Control
MNPs
MNPs-anti-ferritin
Number of cells (%)
100
80
60
40
20
0
Neuron
Astrocyte
Microglia
D
Neuron
Astrocyte
Microglia
Neuron-MNPs
Astrocyte-MNPs
Microglia-MNPs

Figure 5

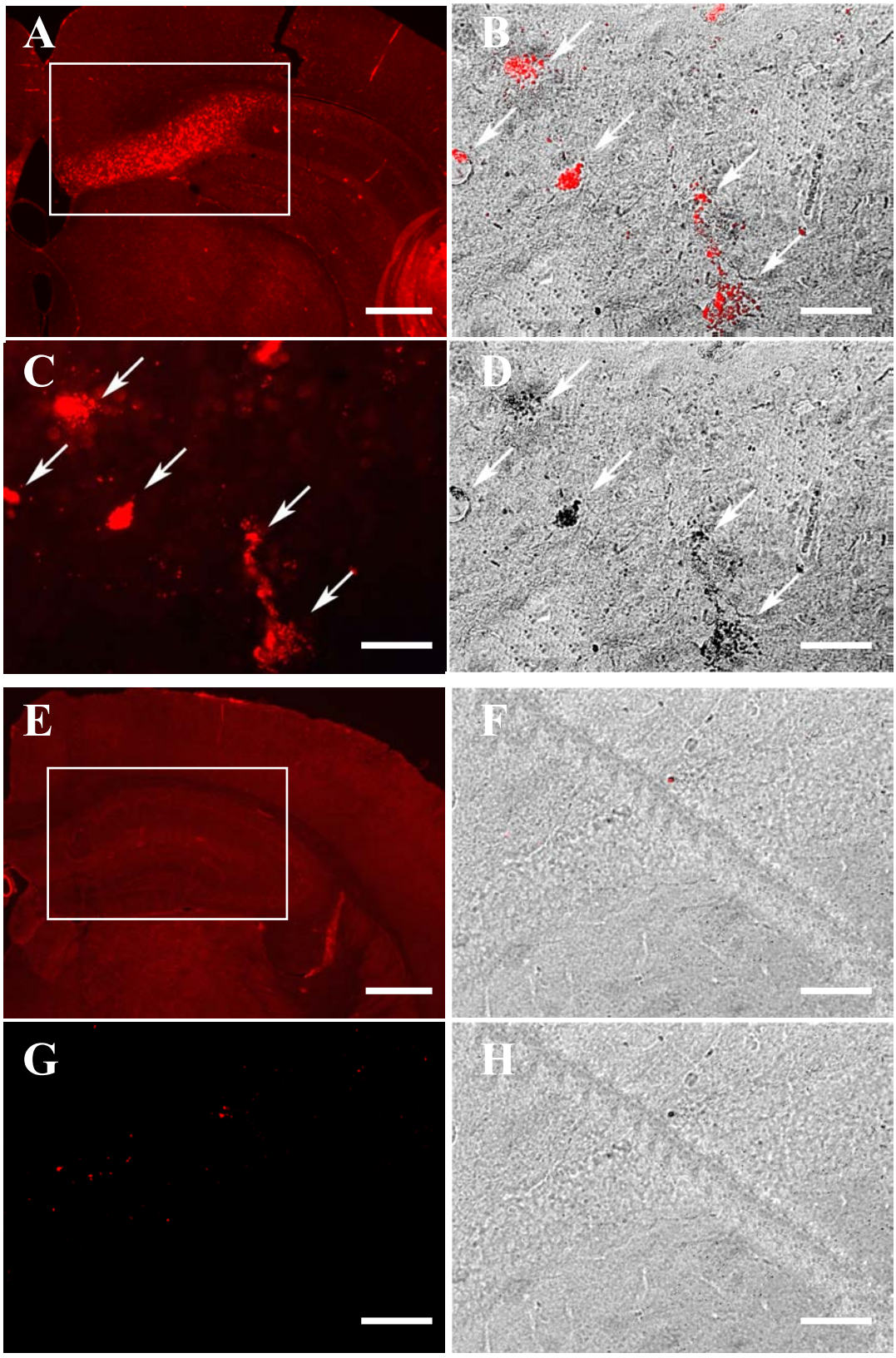

Figure 6

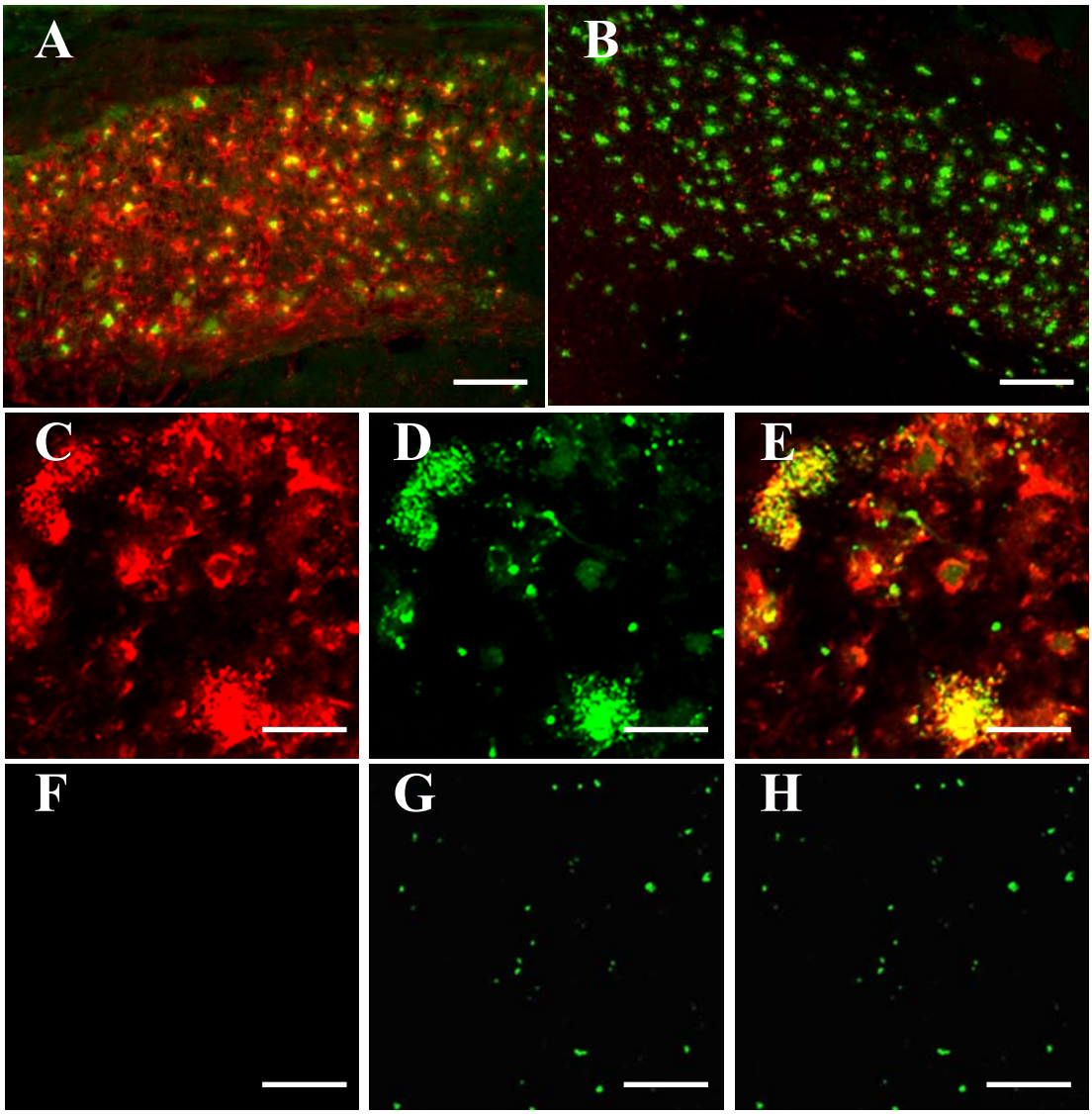

Figure 7

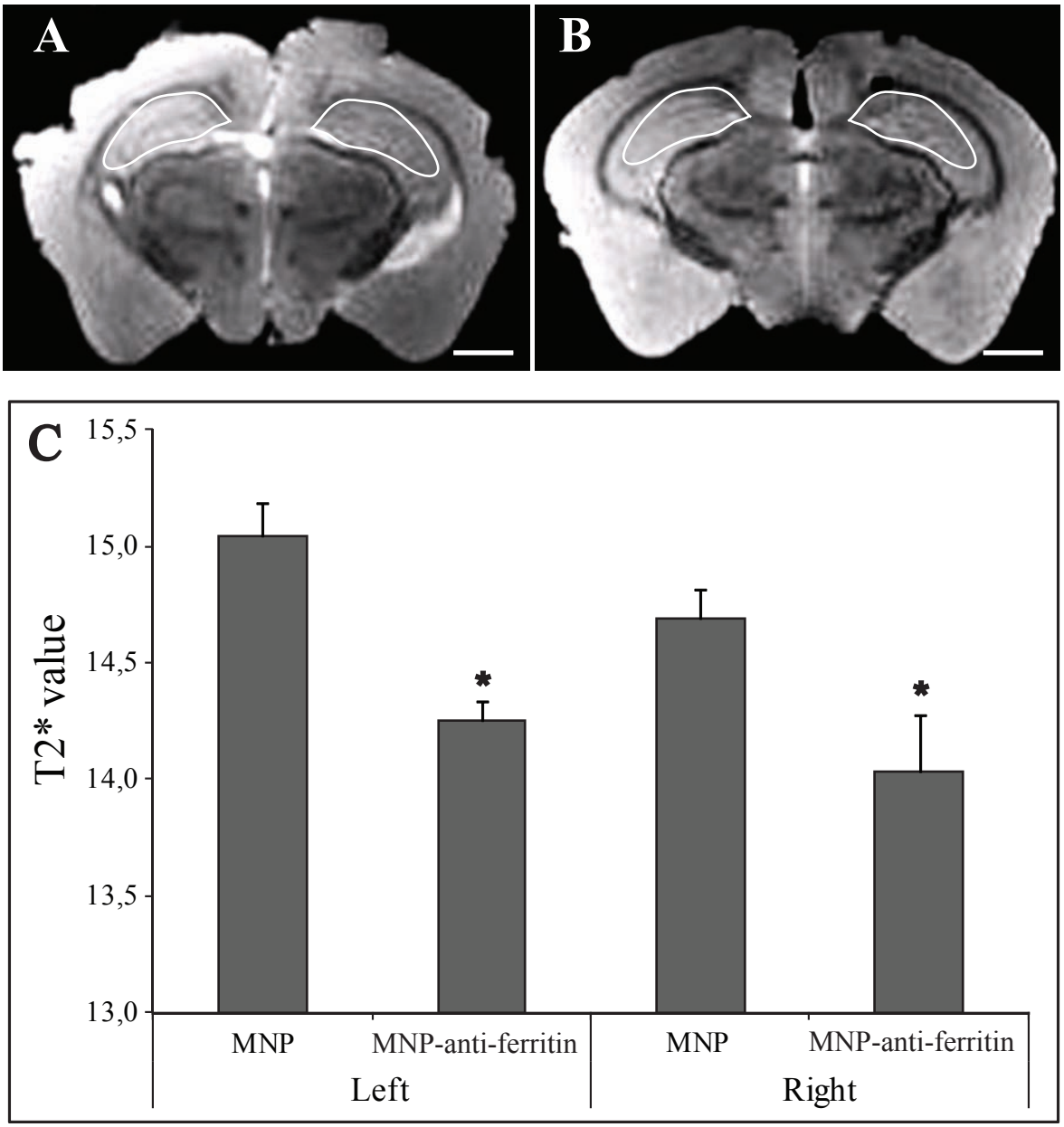
A
B
C
15,5
15,0
14,5
14,0
13,5
13,0
T2* value
*
*
MNP
MNP-anti-ferritin
MNP
MNP-anti-ferritin
Left
Right

Figure 8